Transient Kinetics of *n*-Butane Oxidation to Maleic Anhydride over a VPO Catalyst

Xiao-Feng Huang, Cheng-Yue Li, and Biao-Hua Chen
The Key Laboratory of Science and Technology of Controllable Chemical Reactions, Ministry of Education, Beijing University of Chemical Technology, Beijng 100029, China

P. L. Silveston
Dept. of Chemical Engineering, University of Waterloo, Waterloo, Ontario, Canada

Transient reaction kinetics is usually needed to model the reactor system operated under unsteady-state mode to improve the performance of the catalyst packed in such a reactor system and to match operating conditions of different reaction steps in this system. The transient reaction kinetics of n-butane oxidation to maleic anhydride over a commercial VPO catalyst was systematically studied, using online MS/GC measurements, transient response, and forced periodic operation methods. A simplified scheme with respect to the reaction network is proposed based on the previous studies and the observations in this work. Combining the results on the roles of lattice and adsorbed oxygen in the reaction process with the data obtained in transient response experiments, a transient kinetic model taking account of the oxygen storage and diffusion in the bulk-phase of the catalyst was introduced and its parameters were estimated. The model was examined by the transient response experimental data and time-average concentrations of butane and maleic anhydride under forced unsteady-state operation.

Introduction

The selective catalytic oxidation of hydrocarbon is an important reaction for producing oxygenates, mostly using complex oxides of metals as catalyst and running according to the redox mechanism. The direct oxidation of light alkanes to oxygenates, among all of the selective oxidation technologies, is particularly attractive because alkanes cost less than other feedstock, such as olefins and aromatics. Up to now, the partial oxidation of *n*-butane to maleic anhydride over vanadium phosphorus oxide (VPO) catalyst is the only alkane selective oxidation reaction used in the industry. This reaction system has been studied extensively in recent years because of its significance and because it is representative of the reaction mechanism. Besides the structure of the reaction network (Centi et al., 1988; Xue and Schrader, 1999), the identification of the active phases (Hutchings et al., 1994), and reaction mechanism (Centi et al., 1984; Schuurman and Gleaves, 1994), the kinetic features of the VPO catalyst, which is needed to model the reactor, has been investigated in a series of works. In most of these studies, the steady-state kinetics was experimentally studied, and intrinsic rate equations were proposed based on a triangular reaction network (Escardino et al., 1973; Wohlfahrt et al., 1980; Buchanan and Sundaresan, 1986; Schneider et al., 1987; Sharma et al., 1991; Bej and Rao, 1991). Some information on the reaction rate models is summarized in the Appendix. Recently, Contractor et al. proposed a new unsteady-state reaction mode to synthesize maleic anhydride from *n*-butane by spatial separation of *n*-butane oxidation and VPO catalyst reoxidation in a CFB reactor system and demonstrated its advantages over the traditional technologies (Contractor et al., 1987, 1994; Contractor, 1999). Temporal separation of selective oxidation of *n*-butane and catalyst reoxidation in the fixed-bed reactors of different scales was systematically investigated as a possible alternative method, and obvious improvements in selectivity and yield were observed (Huang, 1999; Huang et al., 2002a,b; 2001). In fact, this is another variety of unsteady-state operation of a chemical reactor system where the catalytic cycle involved is precisely controlled. The selective oxidation of *n*-butane to maleic anhydride in the riser of a CFB reactor system was modeled by Pugsley et al. (1992), based on steady-state reaction rate equation proposed by Centi et al. (1985) and a correction factor corresponding to catalyst deactivation

Correspondence concerning this article should be addressed to C.-Y. Li.

with a decrease in oxygen loading. The initial oxygen loading of the catalyst entering the riser and its effect on the oxidation kinetics were not considered in this work. Golbig and Werther (1997) performed a systematic study of the selective synthesis of maleic anhydride by spatial separation of *n*-butane oxidation and catalyst reoxidation. In their model, with respect to the riser, the butane conversion rate was assumed to be proportional to the *n*-butane concentration and the average oxygen loading, which was experimentally correlated with the regeneration duration in the fluidized-bed regenerator for the catalyst specified.

It should be emphasized that it is very important to take the dynamic behavior of the reaction steps in gaseous and solid phases into account for unsteady-state operation of the chemical reactor system so as to match different reaction steps with respective operation conditions, and to improve the property of the catalyst used in the reactor. Especially for the selective oxidation reaction of butane to maleic anhydride, it is generally accepted that the ability of an oxide catalyst to store lattice oxygen in its bulk phase and release it for surface reactions plays a very important role in the dynamic characteristics of the catalyst (Arnold and Sundaresan, 1987) and of the reactor loaded with this catalyst (Arnold and Sundaresan, 1989). Schuurman and Gleaves (1994) investigated the transient kinetics of *n*-butane oxidation to maleic anhydride over a "reactor-equilibrated" $(VO)_2P_2O_7$ catalyst, using the temporal analysis of the products (TAP) reactor system and roughly lumped the conversion of *n*-butane into a single reaction. It was shown that the selectivity is strongly influenced by the oxidation state of the VPO catalyst and that selectivity increases with the oxygen availability. Further study indicated that the activation energy for the lumped reaction of *n*-butane conversion varied between 53.8 and 98.8 kJ/mol, depending on the oxidation state of the catalyst (Schuurman and Gleaves, 1997).

None of the just-mentioned studies were based on the more rigorous transient reaction kinetics involved in the whole reduction and reoxidation processes of the catalyst, and took no account of the diffusion of the subsurface lattice oxygen. Recently, Barteau and Wang (2000) reported the transient kinetics of the reduction of an equilibrated catalyst in butane/He, and concluded that the reduction of the subsurface layer of the catalyst is not limited by lattice oxygen diffusion. Coulston et al. (1997) explored the transient rate of maleic anhydride formation when either α_1-$VOPO_4/SiO_2$ or $(VO)_2P_2O_7/SiO_2$ catalyst was exposed to *n*-butane, using time-resolved *in situ* X-ray absorption spectroscopy. Their results showed that the rate of maleic anhydride formation is proportional to the rate of decay of the V^{5+} species in the catalyst, even though the rate data were quantitatively not correlated. Huang et al. (2002a) investigated reoxidation kinetics of a VPO catalyst and proposed a transient rate model of this process. Mills et al. (1999) reported the research results on the redox kinetics of the $VOPO_4$ catalysts with *n*-butane and oxygen using the TAP reactor system. For reoxidation processes of reduced $VOPO_4$ catalysts, the transient responses to O_2 step-up could satisfactorily be modeled by a one-dimensional axial dispersion model of the fixed-bed microreactor used in that work, taking the single-surface oxidation reaction with subsurface oxygen diffusion into account. To satisfactorily interpret the transient responses for the reduction processes of the $VOPO_4$ catalysts with *n*-butane, they assumed that the surface lattice oxygen was the only source of active oxygen and proposed a reaction network consisting of three parallel reactions between the surface lattice oxygen and gas-phase *n*-butane to directly form maleic anhydride, CO_2, and CO, taking the lattice oxygen diffusion in the bulk-phase of the catalysts into account.

As a powerful tool for studying the mechanisms and the transient kinetics of heterogeneous catalytic reactions, a transient-response method has been proposed by Bennett (1976), Kobayashi et al. (1974, 1982a,b), and more recent works. The purpose of this work is to develop a transient kinetic model using the transient-response and periodic-operation methods. The model is generally applicable to the unsteady-state oxidation of *n*-butane to maleic anhydride by spatial or temporal separation processes of *n*-butane oxidation and catalyst reoxidation.

Experimental Studies

Catalyst

The catalyst used in this study was a domestic commercial VPO catalyst developed by the Beijing Research Institute of Chemical Technology. It had undergone a 3,000-h steady-state run in a single-tube wall-cooled reactor and gave a selectivity to maleic anhydride of approximately 63—60% at 85—90% conversion. XRD measurement showed that the catalyst was mainly $(VO)_2P_2O_7$. Chemical analysis indicated a P/V ratio of 1.0 and vanadium oxidation state of 4.10. The catalyst packed in the microreactor was crushed and sieved into 60 to 80 meshes.

Experimental setup

The studies for identifying the structure of the reaction network, transient response experiments, temporal separation experiments of selective oxidation and reduction of the catalyst, and forced unsteady-state operation of a fixed-bed reactor were performed with the experimental setup shown in Figure 1. This laboratory system comprised three parts: the gas-blending station for preparing the gas mixture with different compositions, the assembly of the fixed-bed microreactor–electric oven with a multichannel temperature controller and an on-line mass-spectrometer–gas chromatograph analysis system.

The gas-blending station consisted of five mass flowmeter controllers, two three-way switching valves, and one four-way switching valve. The two-position four-way valve was used to switch between the reactant mixtures for the selective oxidation of *n*-butane and reoxidation of the catalyst. The opening of Valve 6 must be preregulated to ensure flow stability before and after switching. Valve VS1, a two-position three-way valve, was used to switch between the standard gas with its composition preblended and He, as the sweeping gas. Valve VS2 was used to switch between the reactant mixture and the sweeping/standard gas.

The main parts of the microreactor assembly are

- Fixed-bed microreactor: 4.7 mm ID; 302 mm length
- Electric oven: 800 W

The temperature of the reaction section was measured with a microthermol couple inserted in its center through a small

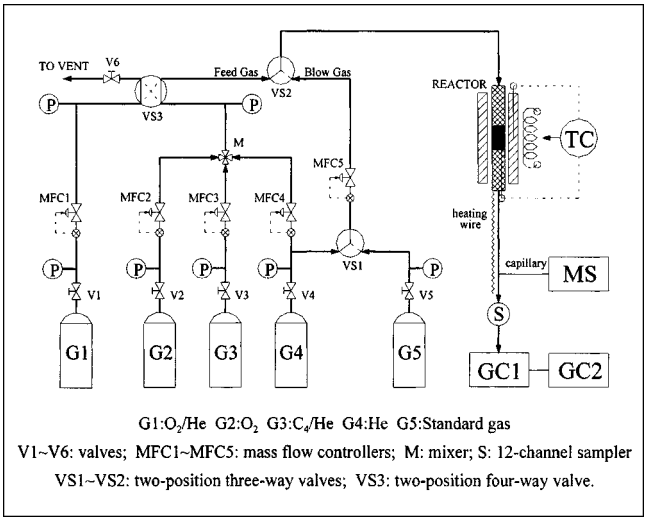

Figure 1. Experimental setup.

jacketed tube and controlled with a temperature-programmable controller. Temperature fluctuation in the reaction section was no more than 1°C, so it was assumed to be an isothermal operation. The reaction section of the microreactor was packed with about 0.6 g of 60/80 mesh catalyst, and quartz chips were loaded in both sides of the reaction section to preheat the feed gas and to stop possible flames when the concentration of butane is higher than its low flammability limit (LFL). The body of the reactor was grounded.

The analysis system consisted of an on-line mass spectrometer, VG70-SE, that was connected by a capillary tube, which was as short as possible, to the microreactor outlet, and a series of two online GCs, which were used to quantitatively analyze the stationary or transient composition of the gas mixture. The first on-line GC was equipped with a 12-channel gas sampler, which could collect 11 samples during the period and analyze them later.

Products analysis

A series of two GCs with a multichannel sampler was used to monitor the transient concentrations of *n*-butane (C_4), CO_2, CO, and O_2. The first GC, with a 3.5-m-long GDX-501 column, was used to analyze C_4H_{10} and CO_2, while the second GC, with a 3.0-m-long 13X molecular sieve column was used to analyze O_2, N_2, and CO. Two gas chromatographs were equipped with thermal conductivity detectors (TCD), and helium was supplied as carrier gas. The signals of the GCs were calibrated with standard gases. The relative correction factor for O_2, CO, CO_2, and *n*-C_4H_{10} were 1.0, 1.02, 0.85, and 0.53, respectively. The tail gas from the GCs was introduced into a water-absorber to collect maleic anhydride, then flowed through a soap-film meter to measure the flow rate. The solution containing maleic anhydride was sampled from the absorber and titrated with the standard solution of NaOH. The stationary and time-average concentrations of maleic anhydride in the product gas could be calculated according to either the titration values of the maleic anhydride solution or the gas-phase concentrations of *n*-butane, CO_2, CO, and O_2, and the flow rates of the feed and tail gases, based on the carbon balance. It was verified that the relative difference between the two methods was less than 3%. This fact suggests that the total acids measured by using the titration method is almost completely maleic acid, even though trace amounts of other species, such as acetic acid and acrylic acid, were also detected by an online mass spectrometer. The transient concentrations of the maleic anhydride in the gas phase involved in the transient-response experiments had to be calculated according to the first method just mentioned. Further details of the analysis are presented elsewhere (Huang, 1999).

Preliminary experiments

Using MS and GC, experiments were performed to determine suitable analytical conditions, to confirm the absence of internal and external diffusion effects on the reaction kinetics and to determine the flow pattern and the hydrodynamic lag time from the reactor outlet to the MS. It was shown that the assumptions of step-change in feed composition and plug flow are acceptable, and that the hydrodynamic lag time from the switching values of feed composition to the detector of the MS was about 20 s at a space velocity of 4,000 h^{-1}.

Experimental procedures

For temporal separation of butane selective oxidation in the fixed-bed reactors, the ratio of butane to oxygen is generally switched between higher and lower valves. To compare the time-average performances of the unsteady-state operation with those of the steady-state operation of industrial wall-cooled fixed-bed reactors, where the feed concentration of butane is about 1.5% and approaches its low flammability limit (LFL) in air, of 1.6% (Crowl et al., 1990), the periodic operation experiment had to be performed by switching the butane concentration between those that were higher and lower than LFL. Therefore, transient kinetic information was needed in the area that is higher than LFL and some transient-response experiments in the area had to be done. It should be emphasized that these experiments can only be undertaken in a microreactor, and some measures must be taken to prevent fires and explosions, for example, adding quartz chips to both sides of the catalyst bed and grounding the reactor body as described in the section on the experimental setup. For the unsteady-state operation of a large-size fixed-bed reactor and with a composition modulated reaction system, it is strongly suggested that the concentration of oxygen in the butane-rich duration should be lower than the minimum oxygen concentration (MOC) required to propagate a flame, such as 10.4% O_2 for a butane–oxygen–inert mixture (Crowl et al., 1990).

Three different types of experiments were undertaken in this investigation. To identify possible intermediates and get a greater understanding of the reaction network scheme, a group of steady-state experiments with a mixture of 3% *n*-butane, 15% oxygen, and balanced helium as feed gas were conducted at 372°C, 402°C, and 440°C, respectively. The samples of product gas were analyzed by GC-MS to detect products in the *n*-butane oxidation reactions. To probe the possible decomposition products of maleic anhydride, a few analytically pure maleic anhydride crystals were packed in a small container situated upstream of the microreactor. The container was placed in an additional oven and heated to subli-

mate the maleic anhydride crystals. Helium gas was passed through the container and into the microreactor where the reaction temperature was kept at 402°C. The effluent of the reactor was also analyzed by GC-MS.

To determine the parameters in the transient kinetic model, two groups of transient-response experiments were carried out at different temperatures or different feed conditions. Three kinds of gas mixture—1.55% C_4 + 21.62% O_2, 2.78% C_4 + 15.10% O_2, and 3.34% C_4 + 22.03% O_2—were used in these experiments, and the temperature varied from 400°C to 430°C. The flow rate was always kept at 20 mL(STP)/min, and pressure in the reactor was kept at 200 kPa. To stabilize and keep the same oxidation state of the catalyst, before each experiment the catalyst was pretreated at 415°C for one hour with 20% oxygen-containing gas, after which a reaction mixture of 1.5% *n*-butane and 20% oxygen was introduced to the reactor for one hour. After the reactor was swept with helium gas, the reaction temperature was regulated to a specified value and the catalyst was reoxidized at this temperature for a given duration with 20% oxygen-containing gas. Finally, the feed was switched to a mixture of butane and oxygen.

The periodic-operation experiment was performed to examine the transient model, typically using the strategy of cycling between 2.78% C_4 + 15.45% O_2 + balanced He and 20% O_2 + balanced He for a period of 6 min at 415°C. An online mass spectrometer was used to monitor the concentration responses and confirm that the cycling steady state was achieved. Then, the reactor effluent was sampled and quantitatively analyzed with GC.

Results and Discussion

Structure of the reaction network

For the steady-state reaction at 372°C, 402°C, and 440°C, and a feed with 3% *n*-butane, 15% oxygen, and balance helium, the major products were found to be carbon oxides, water, and maleic anhydride. Trace amounts of butene, acetic acid, acrylic acid, furan, and benzene were also found. While for an oxygen-poor feed of 12% C_4 + 5% O_2 at 402°C, besides the products just mentioned, trace amounts of 2,5-dihydrofuran and methylbenzene were also observed. However, butadiene, crotonaldehyde, and methyl vinyl keton, which Centi et al. (1984) observed under similar conditions, were not found.

The catalytic decomposition products of maleic anhydride at 402°C were found to be trace amounts of acetic acid, acrylic acid, benzene and methylbenzene, carbon dioxide, and water. Only the small amounts of carbon dioxide and water can be explained by using a maleic anhydride-containing gaseous mixture without oxygen as the feed to the catalytic decomposition. This suggests that a series of deeply oxidized reactions of maleic anhydride occurred.

Observed facts relevant to the kinds and the amounts of the intermediate products from *n*-butane to maleic anhydride, CO_x and H_2O are basically consistent with most of the previous works. Considering that all products, except maleic anhydride, CO_x, and H_2O, appear in trace amounts, it can be seen that this reaction network pattern is factually very similar to those presented by Cavani and Trifiro (1994) and Gleaves et al. (1988), from the viewpoint of a simplifying kinetic representation.

Further sequential transient experiments provided more information relevant to the roles of adsorbed and lattice oxygen, and it was concluded that the surface lattice oxygen and adsorbed oxygen are directly responsible for the formation of maleic anhydride and CO_2, respectively. The adsorbed and lattice oxygen on the surface of the catalyst can be transformed to one another, so the diffusion of the lattice oxygen in the bulk phase of the catalyst will indirectly influence the response behavior of CO_x for a long time under transient reaction conditions. More details can be found in another article (Huang et al., 2002b).

Transient response and period operation

The results of transient responses to step-change in feed composition at different temperatures and different feeds arc shown in Figures 2 and 3. The concentration response of MA was rapid right after switching from oxygen-containing gas to butane-containing feed in each experiment, but it soon declined to a steady level. This suggests the possibility of improving the reactor performance by periodically changing feed composition.

During the periodic-operation experiment, the time-average concentration of each component approached a nearly invariant value after about 20 cycles, which suggested that the cycling steady state was achieved. The transient concentration responses of MA monitored by the on-line mass spectrometer are shown in Figure 4, while the quantitative measurements at cycling steady state by a series of two GCs are shown in Figure 5. The overshoots of MA can be seen in both figures, but the one in Figure 4 is much stronger than that in Figure 5. This probably can be explained by the relatively long time interval between the two samplings in GC measurements, even when the multichannel sampler is used. Even so, the results of the measurement with GC are really the time-average values for a short time. Thus, the measurement by an online mass spectrometer is closer to the real transient response. However, because of the difficulty in

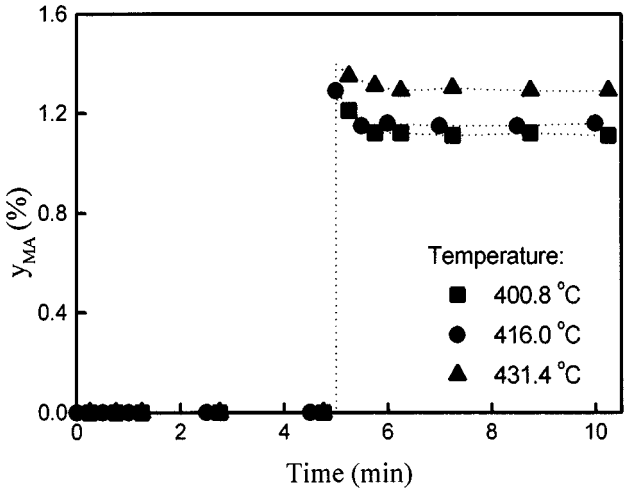

Figure 2. Concentration response of MA to step-change in feed composition at different temperatures.

Feed composition was switched to 1.5%C_4 + 20%O_2 + balance helium after a 5-min reoxidation at different reaction temperatures.

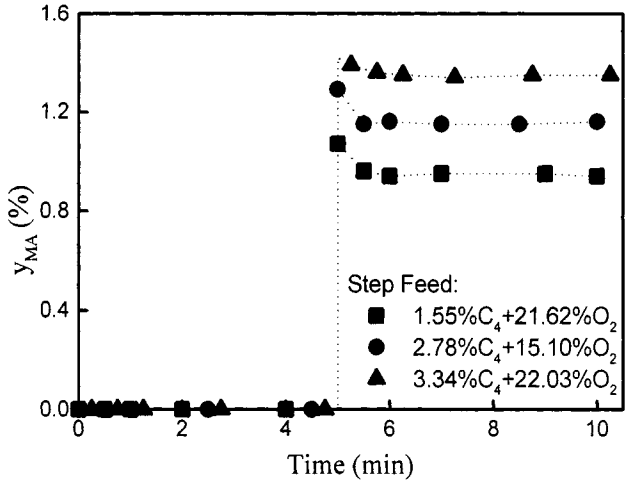

Figure 3. Transient response of MA to step-change in feed composition at different concentrations of butane.

Feed was switched to the compositions given after a 5-min reoxidation at 415°C.

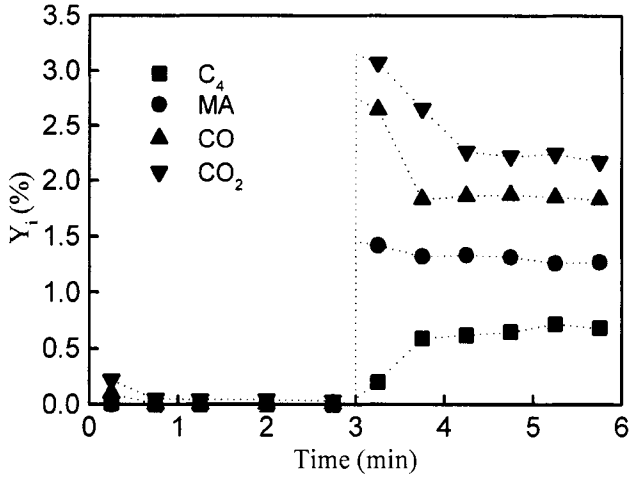

Figure 5. Product concentration at cycling steady state for feed-composition modulation.

Transient concentration of different species in a period duration of 6 min. Feed composition was switched from 20% O_2 + balance helium to 2.78% C_4 + 15.50% O_2 + balance helium at the third minute reaction temperature: 415°C.

quantifying MA by online mass spectrometer, the GC measurement results are still used for estimating kinetic parameters.

Transient kinetics model

As a result of the investigation of transient reoxidation kinetics for the VPO catalyst used in this work, a reoxidation dynamic model, including the following surface reaction steps proposed by Arnold et al. (1989), has been adopted here

$$O_2 + 2(s) \xrightarrow{k_1} 2O(s) \tag{1}$$

$$O(s) + (l) \underset{k'_2}{\overset{k_2}{\rightleftharpoons}} O(l) + (s) \tag{2}$$

Integrating the reoxidation kinetic model with the reaction network pattern and the roles of oxygen species discussed earlier, a set of surface reactions involved in the formation of maleic anhydride can be devised as follows

$$C_4H_{10} + O(l) \rightleftharpoons C_4H_8(l) + H_2O \tag{3a}$$

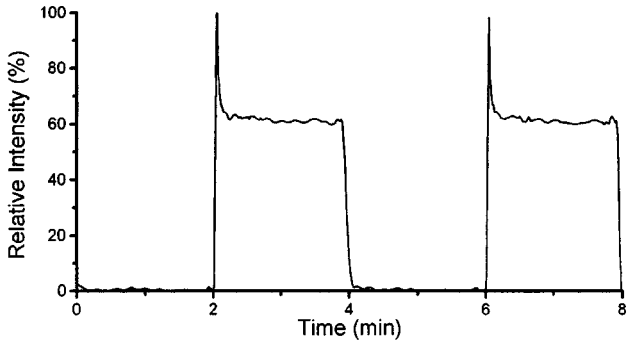

Figure 4. Transient concentration response of MA under periodic operation monitored by online mass spectrometer.

$$C_4H_8(l) + O(l) \rightarrow C_4H_6(l) + H_2O + (l) \tag{3b}$$

$$C_4H_6(l) + O(l) \rightarrow C_4H_6O(l) + (l) \tag{3c}$$

$$C_4H_6O(l) + O(l) \rightarrow C_4H_4O(l) + H_2O + (l) \tag{3d}$$

$$C_4H_4O(l) + 3O(l) \rightarrow C_4H_2O_3(l) + H_2O + 3(l) \tag{3e}$$

$$C_4H_2O_3(l) \underset{k'_4}{\overset{k_4}{\rightleftharpoons}} C_4H_2O_3 + (l) \tag{4}$$

It is well known that the initial oxidation rate of 1-butene is several tens times higher than that of *n*-butane (Cavani and Trifiro, 1994). Moreover, all products except maleic anhydride, CO_x, and H_2O are almost trace amounts, just as we observed in our experiments. This suggests that the surface concentrations of $C_4H_8(l)$, $C_4H_6(l)$, $C_4H_6O(l)$, and $C_4H_4O(l)$ in Reactions 3a–3e can be considered to be zero, and Reaction 3a dominates the sequence of processes from Reactions 3a to 3e. Obviously, this is also the reason why the processes of releasing intermediates from the surface of the catalyst to the gas phase have been left out from the sequence just mentioned. Therefore, by summing all the reactions from Reactions 3a to 3e, a lumping reaction should be obtained as follows

$$C_4H_{10} + 7O(l) \xrightarrow{k_3} C_4H_2O_3(l) + 4H_2O + 6(l) \tag{3}$$

The rate expression of this lumped reaction can be deduced according to the mass action law based on Reaction (3a).

Because MA could be adsorbed on the surface of the catalyst, whereas C_4H_{10} could not be, and the adsorbed oxygen is responsible for the formation of CO_x (Huang et al., 2002b), a set of formation reactions of CO_x can be approximated as follows

$$C_4H_{10} + 9O(s) \xrightarrow{k_5} 4CO + 5H_2O + 9(s) \tag{5}$$

$$C_4H_{10} + 13O(s) \xrightarrow{k_6} 4CO_2 + 5H_2O + 13(s) \tag{6}$$

Table 1. Overall Reaction Scheme and Rate Equations

Reactions	Rate Expression
5	$k_5 y_{C_4} \theta_S$
6	$k_6 y_{C_4} \theta_S$
7	$k_7 \theta_{MA} \theta_S$
8	$k_8 \theta_{MA} \theta_S$

$$C_4H_2O_3(l) + 2O(s) \xrightarrow{k_7} 4CO + H_2O + (l) + 2(s) \quad (7)$$

$$C_4H_2O_3(l) + 6O(s) \xrightarrow{k_8} 4CO_2 + H_2O + (l) + 6(s) \quad (8)$$

Further simplifications are needed to model the transient kinetic behavior of the reaction-diffusion system, owing to the undetermined structure of the elementary step sequence for Reactions 5−8 and the complexity of oxygen diffusion in the bulk phase of the catalyst. The following basic assumptions are adopted to simplify the descriptions of the reaction and transport processes in the fixed-bed microreactor:

(1) The reaction rates of Reactions 5−8 can be expressed as the rates of their controlling steps, as listed in Table 1;

(2) The diffusion rate of the lattice oxygen in the bulk phase of the catalyst is considered to be directly proportional to the difference between θ_L and θ_B; in other words, $r_D = k_D(\theta_L - \theta_B)$;

(3) The axial dispersion in the catalyst bed is negligible, and a one-dimensional plug-flow model for the fixed-bed microreactor can be adopted.

Obviously, the second of these assumptions masks partly the truth. It followed an example where a simplified lumped-parameter model, which included the bulk phase diffusion of the nitrogen atom in an iron-based catalyst, successfully predicted the transient responses to step changes in feed composition and the time-average performance of unsteady-state ammonia synthesis (Li et al., 1985). A more rigorous consideration should lead to a set of PDEs, as was done recently in Mills et al. (1999).

Based on these assumptions, all the rates of eight reactions can be respectively described by the following elementary processes

$$r_1 = k_1 y_{O_2} \theta_{S,V}^2 \quad (9)$$

$$r_2 = k_2 \theta_S \theta_{L,V} \quad (10)$$

$$r_3 = k_3 y_{C_4} \theta_L \quad (11)$$

$$r_4 = k_4 \theta_{L,MA} - k_4 y_{MA} \theta_{L,V} \quad (12)$$

$$r_5 = k_5 y_{C_4} \theta_S \quad (13)$$

$$r_6 = k_6 y_{C_4} \theta_S \quad (14)$$

$$r_7 = k_7 \theta_{L,MA} \theta_S \quad (15)$$

$$r_8 = k_8 \theta_{L,MA} \theta_S \quad (16)$$

The transformation rates of different species in the gas phase, bulk phase, and on the surface are, respectively

$$R_{C_4} = -r_3 - r_5 - r_6 \quad (17)$$

$$R_{MA} = r_4 \quad (18)$$

$$R_{O_2} = -r_1 \quad (19)$$

$$R_{CO} = 4r_5 + 4r_7 \quad (20)$$

$$R_{CO_2} = 4r_6 + 4r_8 \quad (21)$$

$$R_{H_2C} = 4r_3 + 5r_5 + 5r_6 + r_7 + r_8 \quad (22)$$

$$R_{\theta_S} = 2r_1 - r_2 - 9r_5 - 13r_6 - 2r_7 - 6r_8 \quad (23)$$

$$R_{\theta_L} = r_2 - 7r_3 - r_D \quad (24)$$

$$R_{\theta_{L,MA}} = r_3 - r_4 - r_7 - r_8 \quad (25)$$

$$R_{\theta_B} = r_D \quad (26)$$

In these equations the θ_S and $\theta_{S,V}$ are the coverage of adsorbed oxygen sites and vacancies on the surface of the catalyst where oxygen may be adsorbed; θ_L, $\theta_{L,V}$, and $\theta_{L,MA}$ are, respectively, the coverage of surface lattice oxygen, surface lattice oxygen vacancies, and surface lattice oxygen bonded with the precursor of maleic anhydride; and θ_B is a ratio of lattice oxygen concentration in bulk phase to its saturation value. They are assumed to be subject to

$$\theta_S + \theta_{S,V} = 1 \quad (27)$$

$$\theta_L + \theta_{L,MA} + \theta_{L,V} = 1 \quad (28)$$

The $\theta_{S,V}$ and $\theta_{L,V}$ in all of equations with r and R terms can be easily deducted using these two equalities.

Based on the principle of differential mass balances of the species considered, the transient model of the fixed-bed microreactor used in this investigation can elicit a set of partial differential equations with corresponding initial and boundary conditions

$$\frac{\partial N_i}{\partial t} + F\rho_B \frac{\partial N_i}{\partial w} = F\rho_B R_i(y,\theta) \qquad 0 \le t \le T, \qquad 0 \le w \le w_0 \quad (29)$$

$$(N_t)_j \frac{\partial \theta_j}{\partial t} = R_j(y,\theta) \quad (30)$$

$$N_i(t,0) = N_f \times y_{i,f} \quad (31)$$

$$\theta(0,w) = \theta_0 = [0.0,\ 0.1,\ 0.1,\ 0.0]^T \quad (32)$$

where

$$N = \left[N_{C_4},\ N_{O_2},\ N_{MA},\ N_{CO},\ N_{CO_2}\right]^T$$

$$\theta = [\theta_S,\ \theta_L,\ \theta_B,\ \theta_{L,MA}]^T$$

A study of the reoxidation kinetics of the VPO catalyst used in this work showed that the catalyst weight increase after reaction equilibration at 415°C in the mixture, 1.5% C_4 + 20% O_2 + balance He, and a successive reoxidation for several minutes at 400 ~ 430°C in the mixture, 20% O_2 and balance He, as done in the transient-response experiments in this investigation, was about a tenth part of the weight increase of the completely reoxidated catalyst relative to the completely reduced catalyst (Huang et al., 2002a). Therefore, the initial

value for θ_B and θ_L may be approximately considered 0.1 as expressed is Eq. 32.

The inlet concentration of each gaseous component was varied by a step change in feed, while the concentrations of adsorbed components were assumed to be independent of the reactor coordinate and were almost equal to the measurement after the steady-state reaction.

The density of the catalyst bed, ρ_B, and the mass of the loaded catalyst, w_0, are known to be 0.91×10^3 kg/m^3 and 0.5997 g, respectively. The concentrations of active sites were estimated in the reoxidation kinetics studies (Huang et al., 1999)

$$N_{t,\theta_S}=4.73\times10^{-2}\text{mol/kg},\ N_{t,\theta_L}=9.51\times10^{-2}\text{mol/kg},$$

$$N_{t,\theta_B}=3.10\times10^{-1}\ \text{mol/kg}$$

The variable-step finite difference method was used to solve the partial differential equations. It was numerically stable, even when steep concentration gradients occurred in the reactor. In this study, the parameters in the Arrhenius expressions for k_i were estimated from transient experimental data, which spanned the range of feed concentrations and temperatures. A distributed hybrid genetic algorithm developed by Huang (1999) is employed to minimize the objective function defined as

$$RSS=\sum_g\sum_t\sum_i\left\{\left[y^E_{i,g}(t)-y^M_{i,g}(t)\right]/y^M_{i,\max}\right\}^2 \qquad (35)$$

where y stands for the concentration of each component, and g, t, and i stand for the ordinal numbers with regard to the transient-response experiments, the sampled time, and the species in tail gas.

The estimated transient kinetic parameters are summarized in Table 2.

Comparisons between the model predictions of the transient responses to step-change in feed composition and the experimental data are shown in Figures 6 and 7. It can be seen that the model predictions are in good agreement with the experimental data, except for the higher overshoot in the simulation. However, the profiles of the model predictions of the transient-response curves are qualitatively in very good agreement with the MS measurements.

Statistical measures for the proposed model and its relevant parameters were obtained to identify their significance.

Table 2. Estimated Reaction Kinetics Parameters Under Unsteady State

Rate Constant	Exponential Factors ($\text{mol}\cdot\text{g}^{-1}\cdot\text{s}^{-1}$)	Activation Energy ($\text{kJ}\cdot\text{mol}^{-1}$)
k_1	1.402×10^3	56.8
k_2	8.774×10^2	58.9
k_D	4.596×10^4	98.7
k_3	7.038×10^4	66.4
k_4	1.047×10^3	45.4
k'_4	1.260×10^4	67.0
k_5	4.396×10^8	131.5
k_6	7.254×10^8	133.3
k_7	3.866×10^5	87.0
k_8	7.353×10^5	90.4

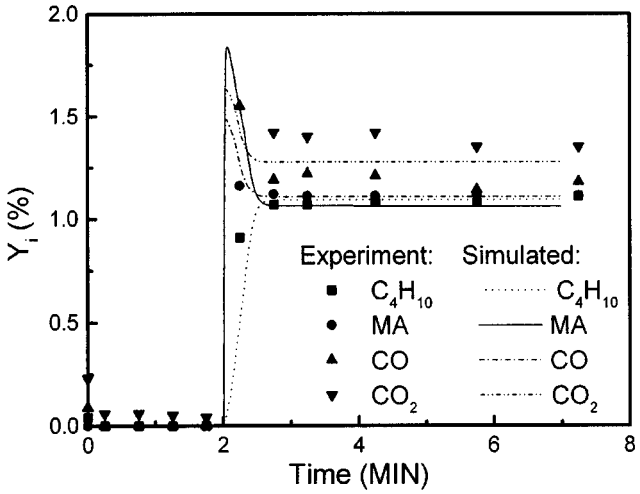

Figure 6. Simulated results based on the bulk inventory model vs. experimental data.

A residual distribution analysis is shown in Figure 8. Almost all of the relative deviations between simulated and experimental transient responses occur in an area limited by two straight lines of $y=(1\pm0.15)x$, where y and x denote simulated and experimental transient responses, respectively. The average relative deviation is 4.01%.

The model was also examined using the data of the forced periodic operation. As shown in Figure 9, the simulated results approaching a cycling steady state are very close to the experimental data.

As shown in Figure 10, a kinetic model that is the same as the previously described model except that the oxygen diffusion in the bulk phase of the catalyst was not taken into account did not fit the transient response data. This suggests that the lattice oxygen stored in the bulk phase of the VPO catalyst and its diffusion play a very important role in transient reaction kinetics, which is a similar conclusion to that drawn by Mills et al. (1999).

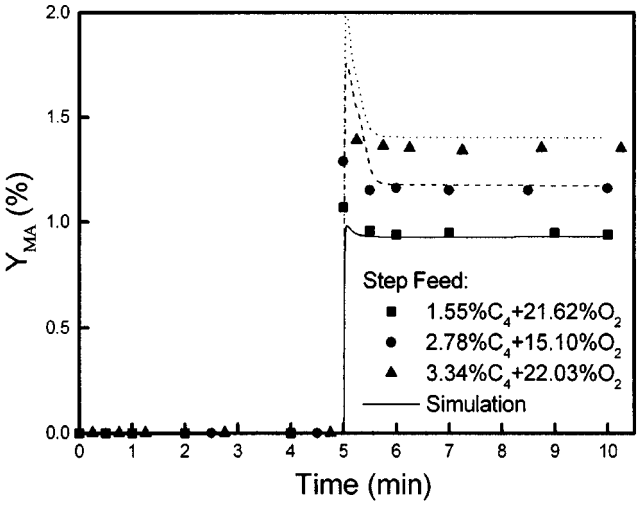

Figure 7. Simulated results vs. experimental data with different feed composition.

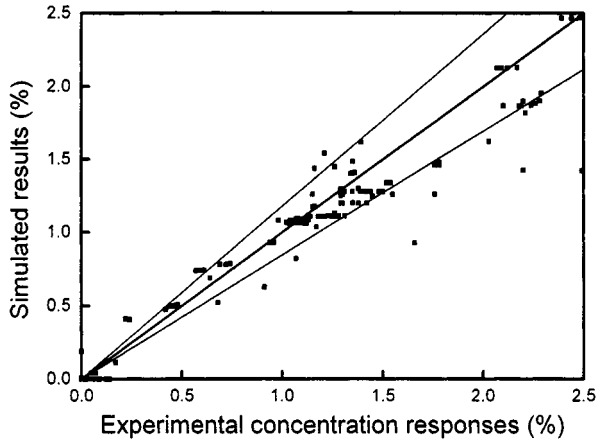

Figure 8. Residual distribution for the model with bulk inventory.

Table 3 shows some results of activation energies obtained in previous studies, using a TAP reactor system. As a comparison, our results gained in this work are also listed. Taking the strong dependence of the activation energy on the oxidation state of the catalyst and the significant differences in the basic assumptions adopted in these works into account, it is believed that there is good agreement between the values of the activation energy with respect to the reaction from *n*-butane to maleic anhydride obtained in these works. As far as concerns the activation energies with respect to other reactions, as indicated in Table 3, there are obvious differences between the results from this work and the previous study. These differences can probably be attributed to the differences in the kinds of the catalyst employed, the structure of reaction network, the kinds of active oxygen, and the forms of reaction rate expressions accepted. It is generally believed that the activation energy of the complete oxidation reaction is greater than that of partial oxidation in a selective oxidation reaction of a hydrocarbon, as seen in some kinetic studies for *n*-butane oxidation to maleic anhydride over VPO catalyst (Bej and Rao, 1991; Buchanan and Sundaresan, 1986). Our results seem consistent with this viewpoint.

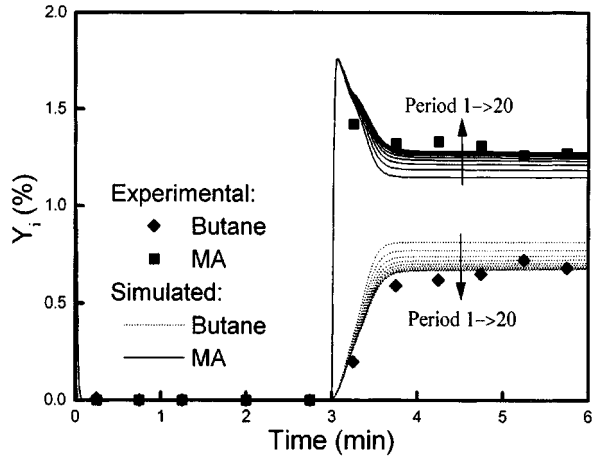

Figure 9. Simulation vs. experimental data under composition modulation.

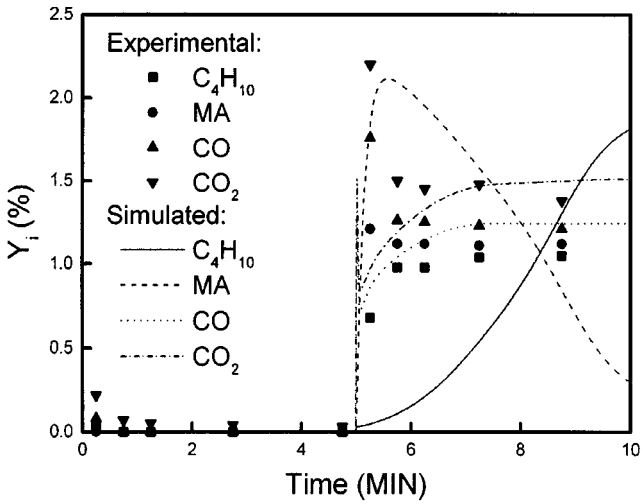

Figure 10. Experimental data vs. simulated results without bulk inventory.

This transient kinetic model was satisfactorily used to predict the transient and time-average performances of the fixed-bed reactors of different scales for maleic anhydride synthesis from *n*-butane, and the relative results will be reported in other articles.

Conclusions

Based on the previous studies and some information with respect to the composition of the reaction products obtained in this work, a reaction network scheme of the *n*-butane oxidation to maleic anhydride is proposed.

Transient-response experiments in which the composition of tail gas using by an online GC equipped with a multichannel sampler were carried out. Starting from the data collected in the experiments, and integrating the results in this work with respect to the reaction network and the roles of different kinds of oxygen in the reaction processes, a transient kinetic model of *n*-butane oxidation to maleic anhydride over a commercial VPO catalyst has been developed. This model considers that the molecular oxygen in the gas phase is dissociatively adsorbed on the surface of the catalyst and can be further transformed to lattice oxygen, and that the *n*-butane in the gas phase reacts directly with the lattice and adsorbed oxygen on the surface to form partial and complete oxidation products, respectively. Moreover, the storage and diffusion of the lattice oxygen in the bulk phase of the catalyst must be taken into account.

A set of transient kinetic parameters has been estimated. It has been shown that the model can fit the data coming

Table 3. Activation Energy of *n*-Butane Oxidation to Maleic Anhydride

	E (kJ·mol^{-1})			
Source	$C_4 \rightarrow MA$	$C_4 \rightarrow CO_2$	$C_4 \rightarrow CO$	$MA \rightarrow CO_x$
Schuurman and Gleaves (1997)	53.8 ~ 98.8	—	—	—
Mills et al. (1999)	71.0	13.0	67.0	—
This work	66.4	133.3	131.5	87.0 ~ 90.4

from the transient-response experiments and predict the data of forced periodic operation very well.

Acknowledgments

The authors gratefully acknowledge the financial support of the National Natural Science Foundation of China under Grant No. 29792073-3.

Notation

E = activation energy, kJ/mol
F = feed flow rate, m^3/s
k = reaction-rate constant, mol/kg cat·s
k_0 = preexponential factor, mol/kg cat·s
k_D = dispersion coefficient, mol/kg cat·s
N = mole flow, mol/s
N_t = moles active sites per kg of catalyst, mol/kg cat
r = transformation rate, mol/kg cat·s
R = total reaction rate, mol/kg cat·s
t = time, s
T = temperature, °C
w = weight of catalyst, kg
y = mole fraction of specified component, dimensionless

Greek letters

θ_B = relative ratio of concentration of lattice oxygen in bulk phase to its saturation value
θ_L = coverage of lattice oxygen on surface, dimensionless
θ_S = coverage of adsorbed oxygen on surface, dimensionless
ρ_B = catalyst-bed density, kg cat/m^3

Superscripts and subscripts

E = estimated data
M = measured data
B = bulk phase
$C4$ = n-butane
f = feed
L = lattice oxygen in surface
S = adsorbed oxygen
V = vacancy

Literature Cited

Arnold, E. W., and S. Sundaresan, "The Role of Lattice Oxygen in the Dynamic Behavior of Oxide Catalysts," *Chem. Eng. Commun.*, **58**, 213 (1987).

Arnold, E. W., and S. Sundaresan, "Dynamics of Packed-Bed Reactors Loaded with Oxide Catalysts," *AIChE J.*, **35**, 746 (1989).

Barteau, M. A., and D. Wang, "Kinetics of Butane Oxidation by Vanadyl Pyrophosphate Catalyst," *AIChE Meeting*, Los Angeles, CA (preprint) (2000).

Bej, S. K., and M. S. Rao, "Selective Oxidation of *n*-Butane to MA, I: Optimization Studies; II. Identi-Fication of Rate Expression for the Reactor; III: Modeling Studies," *Ind. Eng. Chem. Res.*, **30**, 1819 (1991).

Bennett, C. O., "The Transient Method and Elementary Steps in Heterogeneous Catalysis," *Catal. Rev.-Sci. Eng.*, **13**, 121 (1976).

Buchanan, J. S., and S. Sundaresan, "Kinetics and REDOX Properties of Vanadium Phosphate Catalysts for Butane Oxidation," *Appl. Catal.*, **26**, 211 (1986).

Cavani, F., and F. Trifiro, "Catalyzing Butane Oxidation to Make Maleic Anhydride," *Chemtech*., **18**, 4 (1994).

Centi, G., G. Fornasari, and F. Trifiro, "On the Mechanism of n-Butane Oxidation to Maleic Anhydride: Oxidation in Oxygen-Stoichiometry-Controlled Conditions," *J. Catal.*, **89**, 44 (1984).

Centi, G., G. Fornasari, and F. Trifiro, "n-Butane Oxidation to Maleic Anhydride on Vanadium-Phosphorus Oxides: Kinetic Analysis with a Tubular Flow Stacked-Pellet Reactor," *Ind. Eng. Chem. Prod. Res. Dev.*, **24**, 32 (1985).

Centi, G., F. Trifiro, J. R. Enber, and V. M. Franchetti, "Mechanistic Aspects of Maleic Anhydride Synthesis from C_4 Hydrocarbons over Phosphorus Vanadium Oxide," *Chem. Rev.*, **88**, 55 (1988).

Contractor, R. M., H. E. Bergna, H. S. Horowitz, C. M. Blackstone, U. Chowdhry, and A. W. Sleight, "Butane Oxidation to Maleic Anhydride in a Recirculating Solids Reactor," *Stud. Surf. Sci. Catal.*, **38**, 645 (1987).

Contractor, R. M., D. I. Garnett, H. S. Horowitz, H. E. Bergna, G. S. Patience, J. T. Schwartz, and G. M. Sisler, "A New Commercial Scale Process for *n*-Butane Oxidation to Maleic Anhydride Using a Circulating Fluidized Bed Reactor," *New Development in Selective Oxidation II*, V. C. Corberan and S. V. Bellon, eds., Elsevier, Amsterdam, p. 233 (1994).

Contractor, R. M., "Dupont's CFB Technology for Maleic Anhydride," *Chem. Eng. Sci.*, **54**, 5627 (1999).

Coulston, G. W., S. R. Bare, H. Huang, K. Birkeland, G. K. Bethke, R. Harlow, N. Herron, N. Lee, and P. L. Lee, "The Kinetic Significance of V^{5+} in n-Butane Oxidation Catalyzed by Vanadium Phosphates," *Science*, **275**, 199 (1997).

Crowl, D. A., and J. F. Louver, *Chemical Process Safety: Fundamentals with Applications*, International Series in the Physical and Chemical Engineering Sciences, Prentice Hall, Englewood Cliffs, NJ (1990).

Escardino, A., C. Sola, and F. Ruiz, "Maleic Anhydride by Catalytic Oxidation of Butane—I: Mechanism of the Reaction: II. Kinetic Study (at Partial Hydrocarbon Feed Pressure Below 7.5 mm Mercury)," *Ann. Quim.*, **69**, 385, 1157 (1973).

Gleaves, J. T., J. R. Ebner, and T. C. Kuechler, "Temporal Analysis of Products−A Unique Catalyst Evaluation System with Submillisecond Time Resolving" *Catal. Rev.*, **30**, 1 (1988).

Golbig, K. G., and J. Werther, "Selective Synthesis of Maleic Anhydride by Spatial Separation of *n*-Butane Oxidation and Catalyst Reoxidation," *Chem. Eng. Sci.*, **52**, 583 (1997).

Huang, X. F., "Dynamic Kinetic Model of Butane Selective Oxidation to Maleic Anhydride and Its Application," PhD Thesis, Beijing University of Chemical Technology, Beijing (1999).

Huang, X. F., B. H. Chen, B. J. Liu, P. L. Silvestion, and C. Y. Li, "Re-Oxidation Kinetics of a VPO Catalyst," *Catal. Today*, (2002a).

Huang, X. F., B. H. Chen, B. R. Zhao, and C. Y. Li, "Mass Spectrometer Studies for n-Butane Selective Oxidation over a VPO Catalyst," *Chin. J. Chem. Eng.*, (2002b).

Huang, X. F., C. Y. Li, B. H. Chen, C. I. Qiao, and D. H. Yang, "Investigation on Unsteady State Oxidation of N-Butane to Maleic Anhydride in Fixed-Bed Reactors," *Ind. Eng. Chem. Res.*, **40**, 768 (2001).

Hutchings, G. J., A. Desmartin-Chomel, R. Oller, and J. C. Volta, "Role of the Product in the Transformation of a Catalyst to Its Active Phase," *Nature*, **368**, 41 (1994).

Kobayashi, M., and H. Kobayashi, "Transient Response Method in Heterogeneous Catalysis," *Catal. Rev.-Sci. Eng.*, **23**, 1 (1974).

Kobayashi, M., "Characterization of Transient Response Curves in Heterogeneous Catalyst: I. Classification of the Curves," *Chem. Eng. Sci.*, **37**, 393 (1982a).

Kobayashi, M., "Characterization of Transient Response Curves in Heterogeneous Catalyst: II. Estimation of the Reaction Mechanism in the Oxidation of Ethylene Over a Silver Catalyst from the Mode of the Transient Response Curves," *Chem. Eng. Sci.*, **37**, 403 (1982b).

Lerou, J. J., and J. F. Weiher, "N-Butane Selective Oxidation to Maleic Anhydride on a VPO Catalyst," Pittsburgh/Cleveland Catalysis Society Meeting (May 1986).

Li, C. Y., R. R. Hudgins, and P. L. Silveston, "Modeling of Non-Stationary Ammonia Synthesis Kinetics Over an Iron Catalyst," *Can. J. Chem. Eng.*, **63**, 795 (1985).

Mills, P. L., H. T. Randall, and J. S. McCracken, "Redox Kinetics of $VOPO_4$ with Butane and Oxygen Using the TAP Reactor System," *Chem. Eng. Sci.*, **54**, 3709 (1999).

Pugsley, T. S., G. S. Patience, F. Berruti, and J. Chaouki, "Modeling the Catalytic Oxidation of n-Butane to Maleic Anhydride in a Circulating Fluidized Bed Reactor," *Ind. Eng. Chem. Res.*, **31**, 2652 (1992).

Schneider, P., G. Emig, and H. Hofmann, "Kinetic Investigation and Reactor Simulation for the Catalytic Gas-Phase Oxidation of n-Butane to Maleic Anhydride," *Ind. Eng. Chem. Res.*, **26**, 2236 (1987).

Schuurman, Y., and J. T. Gleaves, "Activation of Vanadium Phosphorus Oxide Catalysts for Alkane Oxidation: The Influence of the Oxidation State on Catalyst Selectivity," *Ind. Eng. Chem. Res.*, **33**, 2935 (1994).

Schuurman, Y., and J. T. Gleaves, "A Comparison of Steady-State and Unsteady-State Reaction Kinetics of *n*-Butane Oxidation over VPO Catalysts Using a TAP-2 Reactor System," *Catal. Today*, **33**, 25 (1997).

Sharma, R. K., D. L. Cresswell, and E. J. Newson, "Kinetics and Fixed-Bed Reactor Modeling of Butane Oxidation to Maleic Anhyride," *AIChE J.*, **37**, 39 (1991).

Wohlfahrt, K., and H. Hofmann, "Kinetics of the Synthesis of Maleic Anhydride from n-Butane," *Chem. Ing. Tech.*, **52**, 811 (1980).

Xue, Z. Y., and G. L. Schrader, "Transient FTIR Studies of the Reaction Pathway for n-Butane Selective Oxidation over Vanadyl Pyrophosphate," *J. Catal.*, **184**, 87 (1999).

Manuscript received July 7, 2000, and revision received Aug. 3, 2001.

Appendix. Reaction Rate Models in Butane Oxidation to Maleic Anhydride over VPO Catalysts

Scheme of Reaction Network	Rate Models	Activation Energy, kJ/mol E_1	E_2	E_3	Reference
I. Single reaction butane→MA	Steady-state reaction rates: A. $-r_B = K_1K_2P_B/(K_1 + \alpha K_2P_B)$	56.0			Bej et al. (1991)
	B. $-r_B = kP_B\sqrt{P_{O_2}}/(1 + K_1P_{H_2O} + K_2P_B)$	56.0			Golbig and Werther (1997)
	Unsteady-state reaction rates: C. $r = kC_B$	50.2 ~ 96.3			Schuurman and Gleaves (1997)
II. Triangular reaction network Butane →(1) MA Butane →(3) CO_x MA →(2) CO_x	A. $r_1 = k_iP_B$ $i = 1, 3$ $r_2 = k_2P_{MA}$				Escardino et al. (1973)
	B. $-r_B = r_1 + r_3 = kP_BP_{O_2}^{0.285}/(1 + KP_B)$ $r_2 = kP_{MA}P_{O_2}^{0.285}/(1 + KP_B)$				Wohlfahrt and Hofmann (1980)
	C. $r_i = k_{i,0}\exp\left(\frac{-E_i}{RT}\right)C_B/N$ $i = 1, 3$ $r_2 = k_{2,0}\exp\left(\frac{-E_2}{RT}\right)C_M/N$ $N = 1 + K_1C_B/C_{O_2} + K_2C_M/C_{O_2}$	125.0	180.0	145.0	Buchanan and Sundaresan (1986)
	D. $r_1 = k_1P_B^{0.54}/(1 + K_{MA}P_{MA})$ $r_2 = k_2P_{MA}/(1 + K_{MA}P_{MA})^2$ $r_3 = k_3P_B^{0.54}$	93.1	155.0	93.0	Sharma et al. (1991)
	E. $-r_B = \frac{K_2P_B + K_3K_5P_B/D}{\left(1 + \frac{\alpha K_2P_B}{K_1P_B^0} + \frac{K_5}{D}\right)}$ $D = \beta K_3P_B + \gamma K_4P_{MA}^{0.25}$	103.2	162.5	111.7	Bej and Rao (1991)
	F. $r_1 = k_1K_BC_BC_{O_2}^{0.23}/(1 + K_BC_B)$ $r_2 = k_2C_{MA}/(C_{O_2}^{0.63}/C_B^{1.15})$ $r_3 = k_3C_{O_2}^{0.23}$				Centi et al. (1985)
III. Parallel reaction network Butane →(1) MA Butane →(2) CO Butane →(3) CO_2	Steady-State Reaction Rates: A. $r_1 = k_1(K_{dis}P_{O_2})^{1/2}P_B/(1 + (K_{dis}P_{O_2})^{1/2})$ $r_2 = k_2K_{sorp}P_{O_2}P_B/(1 + K_{sorp}P_{O_2})$ $r_3 = k_3K_{sorp}P_{O_2}P_B/(1 + K_{sorp}P_{O_2})$	72.0	72.1	74.0	Schneider et al. (1989)
	Unsteady-State Reaction Rates: A. $r_{reox} = k_{reox}C_{O_2}(1 - \theta)_{0,S})^{2.0}$	80 ~ 87*			Mills et al. (1999)
	$r_i = k_1C_B\theta_{0,S}^{\gamma_i}$, i = 1, 2, 3 $\gamma_1 = 0.5$ $\gamma_2 = 1.0$ $\gamma_3 = 0.75$	71.0	67.0	13.0	
IV. Five reaction network Butane →(1) MA Butane →(2) CO Butane →(3) CO_2 MA →(4) CO MA →(5) CO_2	A. $r_1 = k_1K_BP_BP_{O_2}/N'$ $r_2 = k_2K_BP_BP_{O_2}/N'$ $r_3 = k_3K_BP_BP_{O_2}/N'$ $r_4 = k_4K_{MA}P_{MA}/P_{O_2}/N'$ $r_5 = k_5K_{MA}P_{MA}P_{O_2}/N'$ $N' = 1 + K_BP_B + K_{MA}P_{MA} + K_{H_2O}P_{H_2O}$				Lerou et al. (1986)

*Activation energy of reoxidation reaction.